Macromolecules

ARTICLE

pubs.acs.org/Macromolecules

Finding the Tube with Isoconfigurational Averaging

Windsor Bisbee, Jian Qin, and Scott T. Milner*

Department of Chemical Engineering, The Pennsylvania State University, University Park, Pennsylvania 16802, United States

ABSTRACT: In an entangled polymer melt or solution, the uncrossability of chains effectively restricts a given chain to move within a confining tube. In this work, we find the tube for a simulated melt of topologically equilibrated rings by averaging chain trajectories over a short time interval, combined with "isoconfigurational" averaging over initial velocities for the same starting configuration. This method allows us to nondestructively image the tube and determine its shape, confining potential, and statistical properties. Using this approach, we investigated the effects of a free surface; we find that tube segments within a few tube diameters of the surface have increased tube diameters by about 25%, and strongly tend to lie parallel to the surface.

INTRODUCTION

For entangled polymer melts and semidilute solutions, the tube model of Doi and Edwards[1] is a well-established basis for developing microscopic constitutive theories of polymer rheology. The tube model represents the effect of uncrossability of entangled chains by confining a given chain to move within a tube. The centerline of the tube is called the primitive path. Motions of the chain perpendicular to the primitive path are confined by an effective potential to transverse displacements of the order of the tube diameter a.

The tube is often regarded as the result of successive discrete entanglements, which are imagined as a sequence of uncrossability constraints involving one other chain, connected by entanglement strands of on average N_e monomers along the given chain. Each entanglement strand is weakly constrained to lie close to the corresponding segment of the primitive path. A sequence of such segments provides a coarse-grained picture of the entire chain.

Within the Doi−Edwards theory, N_e is related to a by $a^2 = N_e b^2$; i.e., the tube diameter is the mean-square end-to-end length of an entanglement strand. The number of monomers N_e between successive entanglements is a fundamental material property of a given melt, and is different for different polymers. The corresponding characteristic time scale for motion of an entanglement strand is τ_e, which is the Rouse time for a strand of length N_e, and thus the time for an entanglement strand to explore its confining tube segment.

The physical significance of the entanglement length N_e or equivalently the tube diameter a is that its value determines the magnitude of the plateau modulus G_∞ of the melt. The plateau modulus and the segmental friction factor are the two microscopic parameters in tube-based theories of melt rheology for both branched and linear chain architectures. Relating N_e or a to experimental data by means of molecular theory has been an area of continued interest.

The Lin−Noolandi (LN)[2,3] ansatz makes a phenomenological connection between the entanglement length and chain dimensions in polymer melts. They posit that an entanglement results when a sufficient number of chain segments cohabit the same volume. This "sufficient number" is asserted to be a universal constant.

The ansatz leads to a proportional relation between the tube diameter a and the packing length l_p, defined as the ratio of the displaced volume of a chain to its mean square end-to-end distance. Fetters et al.[4] gave strong support to the LN ansatz using extensive measurements of plateau moduli and chain dimensions of different polymers. The LN ansatz was later extended to encompass semidilute polymer solutions.[5]

In recent years, properties of the tube have been explored through computer simulation. Everaers et al.[6,7] developed a chain-shrinking algorithm to identify the primitive paths of simulated entangled chains. In this algorithm, the ends of simulated chains are fixed, intramolecular interactions are turned off, and temperature is lowered until the chains are taut. The result is the primitive path seen as piecewise, linear steps between interchain contacts. The average distance between these contacts along a chain is taken to be the tube diameter. Larson et al.[8−10] developed a chain-shrinking algorithm that maintains the chains at fixed tension, arguing that this approach better represents fluctuations in the primitive path length.

Similar chain-shrinking methods were developed by Kröger[11] and Theodorou[12] in the Z program and CReTA algorithms, respectively. These methods use geometric arguments to simultaneously reduce chain contour lengths without allowing chains to cross, and obtain results similar to that of Everaers et al.[6,7]

Despite their success, chain-shrinking methods have definite limitations. The process of drawing the strands tight destroys the detailed geometry of the melt. These methods also introduce a bias toward thinking about entanglements as local binary contacts between chains. Other limitations include the inability to capture tube properties such as width, persistence length, and effective confining potential.

METHOD

To improve upon chain-shrinking methods, this work employs a "nondestructive" method for revealing the tube. Our approach combines time and "isoconfigurational" averaging, i.e., averaging over possible

Received: May 31, 2011
Revised: August 26, 2011
Published: October 31, 2011

chain trajectories to reveal the primitive path without perturbing the chains.

On time scales of order τ_e, monomers in an entangled chain fluctuate inside the tube around some average position, which can be used to define the primitive path. We find the primitive path noninvasively by making many short "movies" of the monomer positions, each starting from the same initial configuration but with different initial velocities or noise histories, and then averaging them together over time. By averaging together many short "movies" from the same starting point, the many different ways the chain can explore the tube are rapidly accounted for, and the effects of the noise history of any particular starting configuration are removed.

This isoconfigurational averaging method has two main advantages over chain shrinking approaches: (1) the end result gives a smooth representation of the primitive path, and (2) the "cloud" of monomer positions around the primitive path reveals the size and shape of the tube.

Prior Results. In their pioneering work, Kremer and Grest[13] used molecular dynamics simulations to collect chain configurations in an entangled melt over short time periods, for a qualitative depiction of tube confinement. Widmer-Cooper and Harrowell[14,15] introduced the isoconfigurational ensemble in their exploration of two-dimensional, glass-forming liquids. In their work, a single initial configuration was evolved over a short time with different initial velocities to show that some particles in a glassy liquid have a greater tendency to move ("dynamic propensity").

More recently, Read, Jagannathan, and Likhtman[16] introduced the idea of defining the primitive path by time-averaging monomer positions over the entanglement relaxation time τ_e, in the context of developing an analytical model for the free energy of the primitive path. Within their exactly solvable model, they concluded that the primitive path has a persistence length of order the tube diameter, and that the chain within the tube is confined by a harmonic potential.

In the present work, we apply directly the idea of defining the primitive path for simulated chains by time-averaging the monomer positions; in addition, we extend this approach by averaging over multiple trajectories generated from the same starting configuration with different noise histories. Any given trajectory with a specific set of monomer initial velocities only explores the tube in one way. As a result, relatively long time averages are required to obtain a smooth primitive path. By averaging many different chain trajectories together, many possible excursions of the chain within the tube are accounted for, revealing the tube without such extensive time averaging.

Use of Rings. In the present work, we study an entangled melt of one or more long ring polymers, in a system with periodic boundary conditions, using molecular dynamics. We introduce Monte Carlo chain-crossing moves that preserve ring identity to topologically equilibrate the system, then turn off the crossing moves to investigate the tube.

Rings afford several advantages for studying entanglement. With crossing moves turned off, entangled rings stay entangled forever, so that a molecule is permanently confined to its tube. We can thus image its tube without any complicating effects from contour length fluctuations, constraint release, or reptation. If the ring is long enough, the local chain geometry and tube properties should be the same as in a system of long, entangled linear chains.

The use of periodic boundary conditions more accurately represents the middle of a melt by minimizing the effects of impenetrable walls. In short, studying rings allows us to focus on the nature of the tube and entanglements within a reasonably sized simulation uncomplicated by chain end effects and tube renewal.

We emphasize that in this work we are not interested in the stress relaxation of a melt of unlinked rings, which is a separate topic of current interest.[17] We study topologically equilibrated rings as a convenient way to study the tube. When we turn off chain crossing in our simulations, we have in effect a random Olympic gel, of permanently entangled rings.

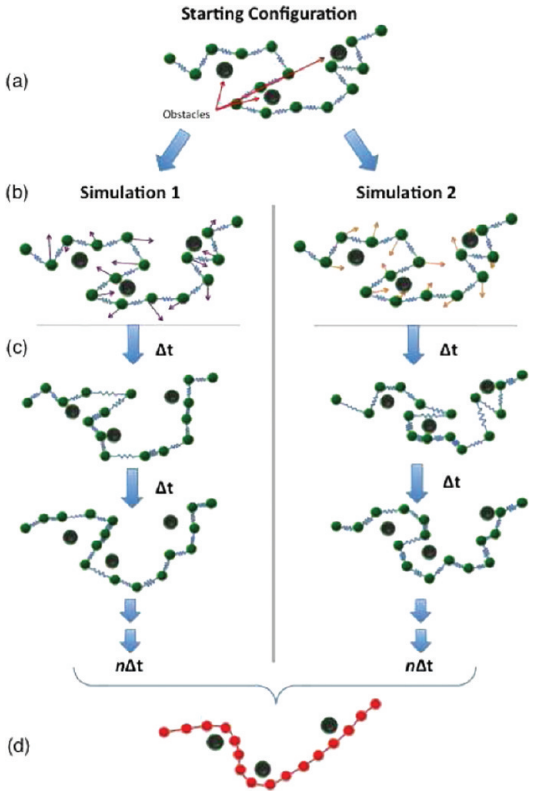

Figure 1. (a) A well-equilibrated polymer chain is taken as the starting configuration. (b) Random initial velocities are assigned in a series of independent simulations. (c) Each simulation trajectory is recorded. (d) Monomer positions are averaged over time and simulation, revealing the centerline of the molecule.

Averaging Procedure. Figure 1 presents a schematic of our averaging procedure. A system of one or more polymer rings is equilibrated through molecular dynamics simulation with Monte Carlo rebridging moves in order to allow the chains to cross themselves and equilibrate their entanglement state.[18,19] Once equilibrated, rebridging is switched off, and the monomer positions are recorded as a starting configuration.

Next, a series of independent simulations are performed, all with the same starting configuration, with random initial velocities assigned to each monomer from a Maxwell−Boltzmann distribution. The duration of the simulations is taken to be several times τ_e, and chain trajectories are recorded at reasonable intervals.

Once data collection is complete, the recorded trajectories are averaged both over time and across simulations to reveal the average position of each monomer. The sequence of average monomer positions define the primitive path. The "cloud" of recorded monomer positions scattered about the primitive path provides a representation of the tube profile. A diameter perpendicular to the primitive path that encompasses a certain fraction of monomer position points is one measure of the tube size.

RESULTS

The following results were generated by equilibrating a single ring of 800 monomers in periodic boundary conditions, using hybrid Monte Carlo simulation with chain rebridging moves for topological equilibration as described in the previous section. Once the system had been topologically equilibrated, an initial configuration was saved, and chain rebridging moves were turned

off. The initial configuration is knotted, as a consequence of the topological equilibration. Then, isoconfiguational analysis was carried out by running 500 independent simulations for 62.5 τ_e from the same equilibrated initial configuration; monomer positions were recorded every $\tau_e/4$.

The Hamiltonian of the simulated chains was represented by truncated Lennard-Jones potentials and harmonic springs. Although the springs are harmonic, the spring constant has been chosen sufficiently stiff that chains essentially never cross each other.[20] We have verified this explicitly in related work in which we compute the topological signature of the system, and confirm that our MD does not result in chain crossings.[21]

The density of the simulated melt was set at 0.7, corresponding to a three-dimensional cubic box of side length 10.5. The simulations were performed on a single processor, and it takes less than 2 days to get 500 isoconfiguration sequences for the 800 monomer system. The MD simulations were performed in the NVE ensemble with an appropriately short time step, although NVT simulations with a Nose−Hoover thermostat gave equivalent results.

We chose to simulate single long self-entangled rings, or only a few rings, for several reasons. The isoconfigurational averaging procedure is computationally intensive, as it relies on multiple (albeit short) MD simulations; thus there is an incentive to use a system that is as small as possible. Our interest is in studying the properties of the tube, which is a local consequence of uncrossability, as close as possible to the limit of a melt of long entangled chains, without effects of ends or finite chain length.

Thus, it is better to study one or a few very long entangled rings, than a larger number of shorter rings. Indeed, if we make the rings too short, they would fail to entangle with each other very much, even if allowed to cross. The relevant measure of system size for our purposes is how many entanglement strands are present; for our single ring of 800 monomers, this turns out to be about 12.

Even though we simulate one or a few rings only, we still expect that screening of excluded volume interactions leads to ideal random-walk chain conformations. We have verified this explicitly for our simulations, observing the equilibrium fluctuations in the radius of gyration while chain rebridging moves are active as an indication that topological equilibration is progressing. Indeed, we find radii of gyration for our rings that are completely consistent with what would be inferred from observed chain dimensions for equilibrated linear melts. When rebridging is turned off, the radius of gyration becomes quenched.

Finally, we note that in prior work on chain shrinking methods applied to entangled linear melts, heuristic attempts were made to assess the importance of preserving uncrossability of a chain with its own distant monomers, which was found to have a small effect on the inferred value of N_e.[7] In contrast, in the present work, because for computational efficiency we simulate only one or a few rings, it is essential to enforce uncrossability of a ring with itself.

Averaging Time. The primitive path in our approach depends on the averaging time τ_a. For efficiency, we would like to take τ_a as short as possible, while still representing the tube well. Clearly the averaging time must be at least τ_e, or else the single initial configuration will not have time to explore the tube even locally.

Averaging times well in excess of τ_e permit the chain to equilibrate by Rouse motion over larger regions of the tube; in principle, this should have the effect of equilibrating contour length fluctuations within the tube, which we may wish to average over.

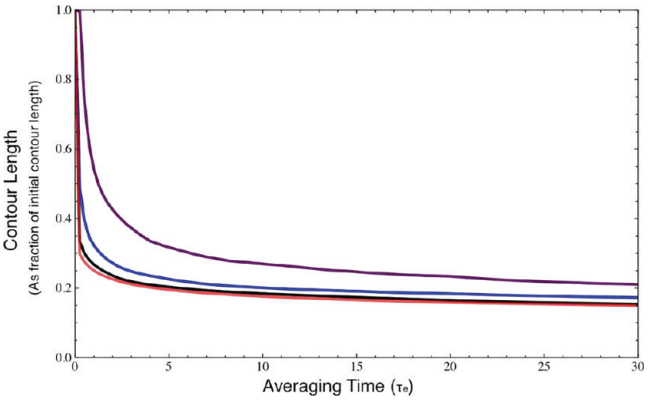

Figure 2. Primitive path contour length versus averaging time, in units of τ_e. The different lines represent from top to bottom, the averages of 1, 5, 25, and the full 500 simulations, respectively.

However, there is a practical difficulty that arises from our prescription for the primitive path for long averaging times. Namely, that tightly curved portions of the path tend to be "rounded off"; as the monomer with average position at the apex of a curve reptates back and forth past the apex on the curved path, the monomer average position falls below what should properly be the tube centerline, defined by the cloud of monomer positions regardless of monomer index.[22]

Fortunately, it turns out that with isoconfigurational averaging, choosing τ_a equal to a few times τ_e gives a very smooth tube, with little of the above-described rounding-off effect. To investigate this behavior, and guide in choosing the averaging time τ_a, the contour length versus τ_a was examined.

Figure 2 displays the dependence on averaging time τ_a of the length of the primitive path as a fraction of its initial value, for different numbers of isoconfigurational trajectories. The contour length decreases quickly at first as short-wavelength modes smooth out, then more slowly, approaching its limiting value. The time-dependence is reminiscent of the Rouse model stress relaxation function, but depends in detail on the particular mode amplitudes in the initial configuration.

The curves in Figure 2 from top to bottom represent the contour length decrease of the average of n isoconfigurational simulations, for n = 1, 5, 25, 500, respectively. These results illustrate the importance of using many simulations instead of just averaging over time. The top curve, representing the time average of one isoconfigurational trajectory, takes much longer to relax toward a limiting value than for the average of 5, 25, or 500 simulations.

From the figure, it is evident that an isoconfigurational average over between 5 and 25 or so trajectories is a sufficient number to give a rapid smoothing of the primitive path; for example, with five trajectories averaged, we reach the same average path length in $5\tau_e$ that averaging over a single trajectory achieves in about $30\tau_e$. Note however that the amount of CPU time required for the two calculations is about the same; the advantage of isoconfigurational averaging is that it provides a more nearly instantaneous, "time-local" view of the tube and its properties.

The relaxation of the contour length of the isoconfigurationally averaged primitive path as a function of averaging time τ_a for $\tau_a < \tau_R$, can be described by the Rouse model. The

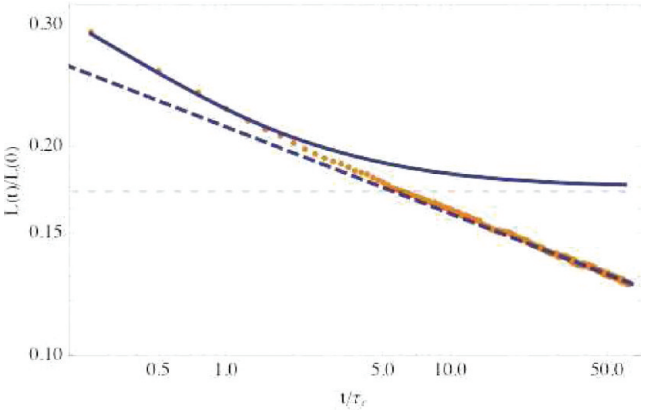

Figure 3. Log−log plot of primitive path contour length (points), versus Rouse model prediction (solid curve), with thin dashed line indicating limiting contour length (see main text). Thick dashed line, $t^{-1/8}$ power law.

isoconfigurational averaging eliminates the effect of variations in the noise history on the primitive path and hence its decreasing contour length; what remains is the relaxation of the particular Rouse amplitudes of the initial primitive path.

The short wavelength Rouse mode amplitudes of the initial primitive path decay exponentially, with time constant τ_p for the pth mode given by the Rouse expression appropriate for ring polymers

$$\tau_p = \frac{\zeta b^2}{12\pi^2 k_B T}\frac{N^2}{p^2} \quad (1)$$

in which b is the statistical segment length and ζ is the monomeric friction factor. However, modes of the primitive path with wavelengths well in excess of N_e do not relax, as they are permanently constrained by entanglements.

To represent this crossover in relaxation behavior between the relaxing short wavelength modes and persistent long wavelength modes, we write the time dependence of the pth Rouse mode in the primitive path in terms of a phenomenological function as

$$f_p(t) = \frac{1-\tanh((p-p_c)/w)}{2} + \frac{1+\tanh((p-p_c)/w))}{2}\exp(-t/\tau_p) \quad (2)$$

in which the cutoff Rouse mode p_c and crossover width w are parameters. We then evolve the primitive path forward as a function of averaging time t by transforming to Rouse modes, applying factors of $f_p(t)$, and transforming back to real space, whereupon we can evaluate the contour length by direct summation.

The curve shown in Figure 3 was obtained in this way. The time scale τ_p is not fitted, but computed from eq 1, with the statistical segment length $b = 1.41$ determined from equilibrium chain dimensions for our bead−spring model, and the friction factor ζ inferred from center of mass diffusion coefficients for simulations of unentangled linear chains.

For the cutoff mode and width, we used $p_c = 11$ and $w = 7$, which values were adjusted by hand to give a reasonable description of the simulation results. The value $p_c = 11$ is consistent with our expectation: it corresponds to a cutoff wavelength of $N/11 = 73$ beads, which is close to the entanglement length 67 we obtain from chain-shrinking methods. (The thin dashed line in Figure 3 indicates the limiting primitive path contour length $L_\infty = 138$ calculated using $N_e = 67$ and the usual Doi−Edwards expressions, i.e., $L = Nb^2/a$ with $N = 800$, $b = 1.41$, $a^2 = N_e b^2$, and $N_e = 67$.)

Figure 3 displays a log−log plot the fractional contour length versus time, in which it is evident there are two regimes for relaxation of the primitive path contour length. The first regime, up to a few times τ_e, is well described by our model; the second, for longer averaging times, shows a primitive path contour length decaying as a power law $t^{-1/8}$.

This decaying contour length would appear to contradict our claim that the primitive path relaxes to a fixed shape with increasing averaging time. In fact, this power law decay is an artifact of our averaging process. When the averaging time well exceeds τ_e, the shape of the "cloud" of locations for each monomer extends far enough that its shape becomes curved, following the curved primitive path.

Then, the average position of the monomer (center of mass of the cloud) no longer resides on the primitive path, but is displaced toward the center of curvature. Thus, the primitive path defined by the average monomer positions tends to "cut the corners" of the true primitive path, shortening its length.[22]

We can construct a scaling argument to understand the observed power law. For times t between τ_e and the Rouse time τ_R, a monomer on a chain confined to a tube randomizes its arclength position s along the primitive path with a variance $\langle \Delta s^2 \rangle$ scaling as $N_e^2(t/\tau_e)^{1/2}$. (The corresponding spatial displacement, along the random-walk contour of the primitive path, has a variance $\langle \Delta R^2 \rangle$ scaling as $(s/N_e)a^2$, or $\langle \Delta R^2 \rangle \sim (t/\tau_e)^{1/4}$, which is the usual $t^{1/4}$ regime of monomer mean-square displacement when the effects of tube confinement on Rouse modes are first felt.)

As the positions of monomers randomize along the primitive path, the path becomes smoother. When the monomers are randomized over a range of arclengths s, the primitive path originally of N/N_e steps of size a is replaced by a smoother path of N/s steps, with size of order the mean-square end-to-end distance of a path segment of length s, which scales as $(s/N_e)^{1/2}a$. The end result is that the smoother primitive path contour length $L(t)$ scales as $(N/s)(s/N_e)^{1/2}a$, or $L(t/\tau_e)^{-1/8}$, as we observe.

In following sections, we take $\tau_a = 10\tau_e$ as a reasonable choice for averaging time; any choice in the range $5\tau_e < \tau_a < 30\tau_e$ would lead to similar results, within a factor of $3^{1/8}$ or about 15%. We shall discuss in the conclusions (and pursue in future work) an improved scheme for determining the centerline from the "cloud" of positions, which mitigates the "corner-cutting" artifact described above.

Path and "Cloud". Figure 4 shows the primitive path and "cloud" of monomer positions resulting from isoconfigurational averaging of one self-entangled molecule of 800 monomers. The primitive path is smooth, and the tube itself can be seen by inspecting the shape of the cloud of monomer positions surrounding the centerline. In Figure 4, the primitive path is "unfolded" across periodic boundaries into an "extended zone" representation, so that the tube can be seen more clearly. In reality, the ring is contained in the periodic confining box (shown as a smaller black box in the figure), where it is entangled with its periodic images. Finally, note that the apparent variation in density of the monomer cloud is only due to the viewing angle relative to the direction of the primitive path. When viewed from other directions, it is evident that the cloud is rather uniform along the primitive path in both density and dimension.

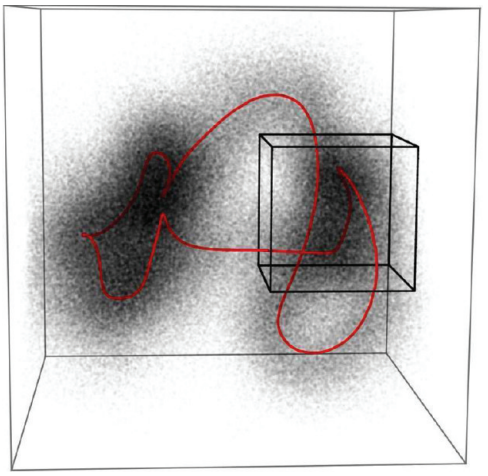

Figure 4. Isoconfigurational primitive path (red) shown with all collected monomer positions for $\tau_a = 10\tau_e$. The periodic confining box is indicated as the small cube.

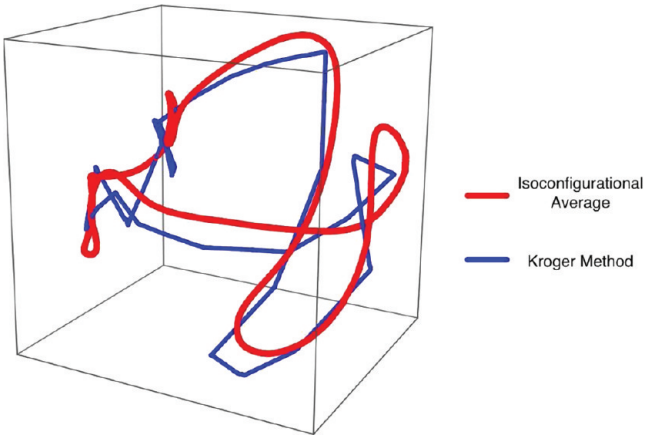

Figure 5. Isoconfigurational ensemble primitive path compared to result from modified Kröger algorithm.

We can compare the primitive path obtained from isoconfigurational averaging to that found by chain-shrinking methods, by applying a modified Kröger algorithm to the same starting configuration. Note that most chain shrinking algorithms necessarily involve chain self-crossing in the process of obtaining primitive paths; the Kröger method alone among previous chain-shrinking approaches can be conveniently modified in a way that is guaranteed to prevent chains from crossing themselves. Since chain self-entanglement is essential in our system, we implemented a modified Kröger method for our comparison.

Note that because our rings are self-entangled with periodic boundary conditions, there is no need to fix the positions of any beads when implementing the modified Kröger method. The uncrossability of the chains and the closure of the rings suffice to prevent the chains from shrinking to a point as the paths are smoothed.

Figure 5 shows a comparison between the Kröger method and the isoconfigurational analysis. Both primitive path representations trace generally the same shape through space. However, the isoconfigurational primitive path is smooth and continuous, while the Kröger result is a coarse-grained approximation.

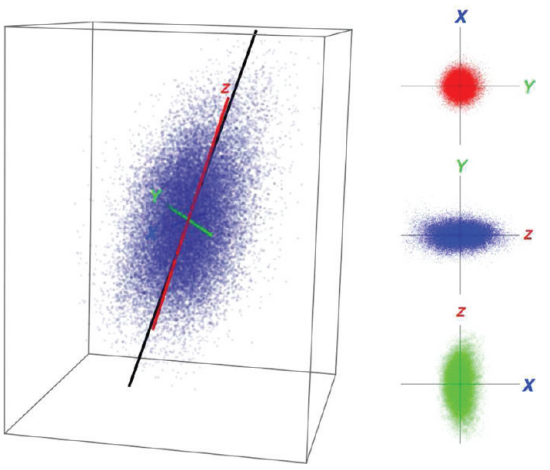

Figure 6. Gyration tensor analysis of isoconfigurational data. Red, green and blue axes represent principal axes of ellipsoid that describes data. Black line represents the direction of primitive path. At right are projections of data points down respective principal axes.

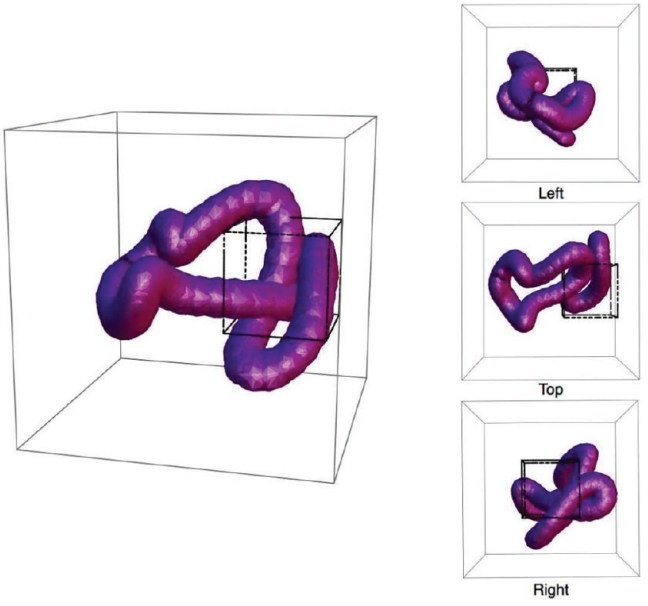

Figure 7. The tube visualized as a series of selected ellipsoids. The confining box is indicated as the small cube.

Indeed, suppose we consider a system in which the rings were so short as to be largely unentangled even when allowed to cross. This will certainly be the case for rings somewhat shorter than N_e. After ring-crossing is turned off, such a system would have almost no permanent entanglements, consisting essentially of a melt of short unlinked rings. The configurational relaxation time for such rings will be somewhat less than τ_e. If we apply isoconfigurational averaging to such a system, within a few times τ_e, each ring will explore a full set of configurations, and the "clouds" of monomers will be indistinguishable, each spread out over the entire region circumscribing the ring. The average monomer positions will all tend to lie at the same place, and the primitive paths so defined will shrink nearly to points, which is the signature of an unentangled system.

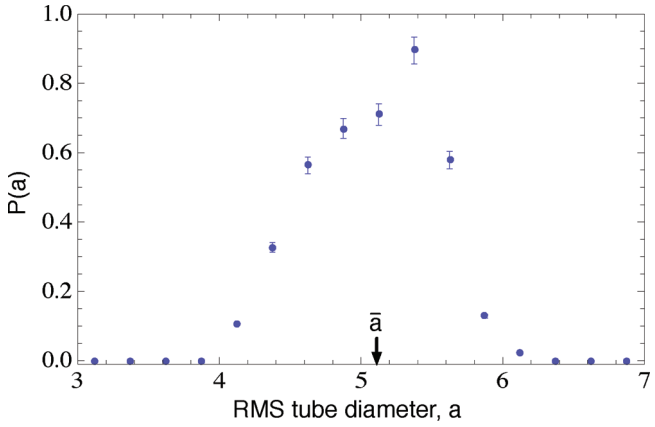

Figure 8. Tube diameter probability distribution, with mean tube diameter $\bar{a}$ indicated. (Results for averaging time $\tau_a = 10\tau_e$.).

Gyration Tensor Analysis. The shape and size of the tube can be found by examining the cloud of monomer positions; for example, we may determine a radius around the centerline that contains a certain density of monomer positions. The tube radius along the primitive path is obtained from the gyration tensor of the cloud for each monomer around its average position.

Figure 6 shows the results of the analysis for a randomly selected monomer, for an averaging time τ_a equal to $10\tau_e$. The cloud takes the form of a prolate ellipsoid, as confirmed by views along the gyration tensor principal axes. The longest principal axis is aligned with the tangent of the primitive path at that monomer, consistent with unhindered motion of the molecule along the path of least resistance within the tube. The two shorter principal axes define the tube radius, taken as the root-mean-square of the standard deviation in each principal direction.

Repeating this analysis for all monomers, a picture of the tube emerges as the collection of the ellipsoids. Figure 7 shows this representation, in which it can be seen that the tube is quite uniform in radius along its length, expanding only slightly in places where the primitive path is highly curved.

Tube and Path Properties. From the primitive path and surrounding cloud of monomer positions, several local and average measures of the tube can be defined. They are (1) the local tube diameter a defined above and its average $\bar{a}$ along the primitive path, (2) the length of a step along the primitive path, defined by $L = (N/N_e)\tilde{a}$, where L is the length of the primitive path, and (3) the persistence arclength l_p of the primitive path.

Within the simple model of Doi and Edwards of the primitive path as a freely jointed random walk of step length a, a would equal $\tilde{a}$, and l_p would equal N_e (see below). But for the physical primitive path, smooth and with a persistence length, all of these quantities should be expected to be different, by factors of order unity.

In addition to the above lengths, another important quantity is the shape of the distribution of monomer positions about the centerline, from which an effective confining potential can be inferred. Below, we discuss and compare all these properties.

Figure 8 displays the probability distribution for the tube diameters (by convention, twice the tube radius defined from standard deviation along the two minor principal axes of the cloud). The figure shows the extent of variation in the local tube size, which is a smallish fraction of the average tube diameter $\bar{a} = 5.1$.

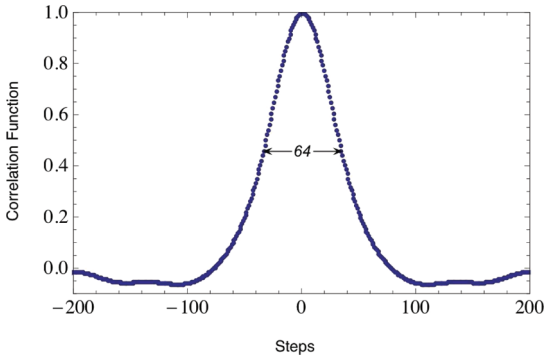

Figure 9. l_p measured by plotting a directional correlation function against monomer steps from a given starting point.

From Figure 3, we see that the primitive path length L shrinks on averaging to about 0.15 of its initial value, which for a ring of 800 monomers is essentially $L_0 = 800$. Thus, the length of the smooth primitive path is about $L = 120$. With a nominal value of $N_e = 67$ from chain-shrinking analysis for this system, which gives N/N_e of about 12, we infer a primitive path step length $\tilde{a}$ of about 10. Since as we shall see the primitive path is slightly semiflexible, it is not surprising that $\tilde{a}$ so defined is somewhat larger than the average tube diameter $\bar{a}$.

Finally, we can measure the persistence arclength l_p of the primitive path, i.e., the number of monomers over which the tangent to the primitive path becomes uncorrelated with its value at some starting monomer. The persistence length is another good measure of the tube diameter, in the sense that for the simple model of the primitive path as a sequence of uncorrelated steps of arclength N_e, the tangent persistence length is also N_e.

Figure 9 displays the tangent−tangent correlation function $C(s - s')$, given by $C(s - s') = \langle n(s).n(s')\rangle$, for the primitive path as a function of monomer separation $s - s'$ along the ring. We can define a measure of the persistence arclength by measuring the full width at half-maximum of the correlation function, which results in a value of $l_p = 64$ monomers. This is quite close to the entanglement length of $N_e = 67$, obtained for this system using chain-shrinking methods.

We have not attempted to fit the shape of the tangent−tangent correlation function in detail to extract a persistence length, in part because our statistics suffer from having only examined a small number of primitive paths. Note that the tangent−tangent correlation function of a chain in a melt has recently been shown to have a power-law tail scaling as $|s - s'|^{-3/2}$ as a result of residual intrachain correlations, rather than the often-assumed exponential decay.[23] The primitive path tangent−tangent correlation function would presumably also have a weak power-law tail of the same form.

The different measures of the tube diameter defined above can be compared in various ways; for example, we can compare the mean square end-to-end distance of a strand of length N_e, which with the observed statistical segment length $b = 1.41$ gives a length of $(1.41)(67)^{1/2} \approx 11.5$, with the tube diameter a and the primitive path step length $\tilde{a}$. Evidently the tube is somewhat smaller than the strand end-end length, which in turn is almost the same as the primitive path step length, consistent with a slightly semiflexible primitive path.

By examining the shape of the cloud of monomer positions around the primitive path, we can infer the effective confining potential $U(r)$ that governs transverse excursions of the chain in

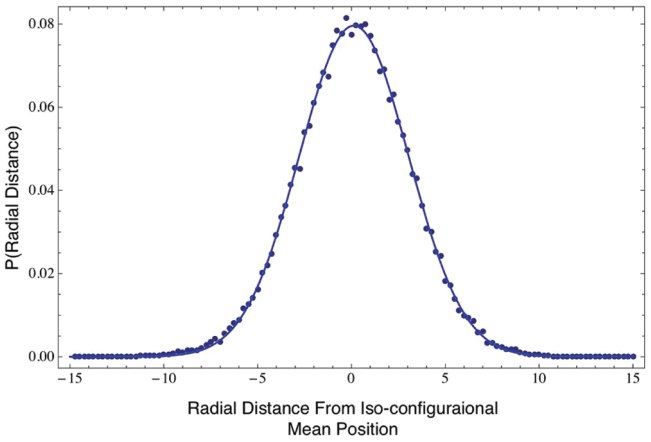

Figure 10. Gaussian probability distribution of radial displacement for a given monomer from its isoconfigurational mean position. The variance σ is 2.45, corresponding to a tube diameter of 4.90.

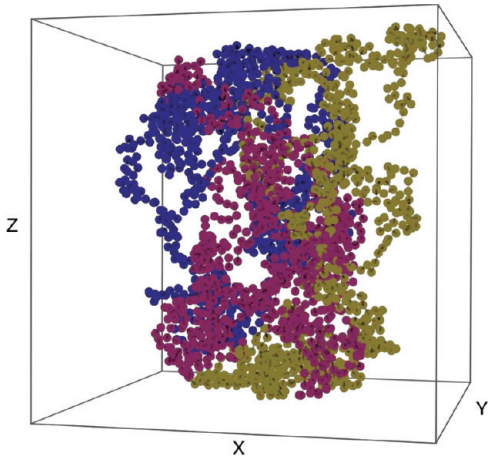

Figure 11. Simulation box, containing three polymer rings. It is periodic in the x and y directions and finite in the z direction, as an representation of a slab of melt.

its tube. From the cloud of positions for each monomer, the displacements from the corresponding point on the primitive path are found, and projected into the plane orthogonal to the long principal axis of the cloud (which lies parallel to the primitive path). We then obtain the probability distribution for displacements along either of the two shorter principal axes. The probability distribution that results for a typical monomer is shown in Figure 10.

This distribution measures the "softness" of the confining tube, in terms of the likelihood that a monomer is found to be a certain distance from its mean position. The distribution is Gaussian, which indicates that the confining potential is harmonic:

$$P(x) = Ae^{-\frac{(x-\mu)^2}{2\sigma^2}} \quad (3)$$

where A, μ, and σ are fitted constants. For the particular monomer distribution in Figure 10, we find a tube radius $\sigma \rightarrow 2.45 \pm 0.03$., corresponding to a local tube diameter of $a = 2\sigma = 4.9$, which is a typical diameter consistent with the distribution in Figure 8.

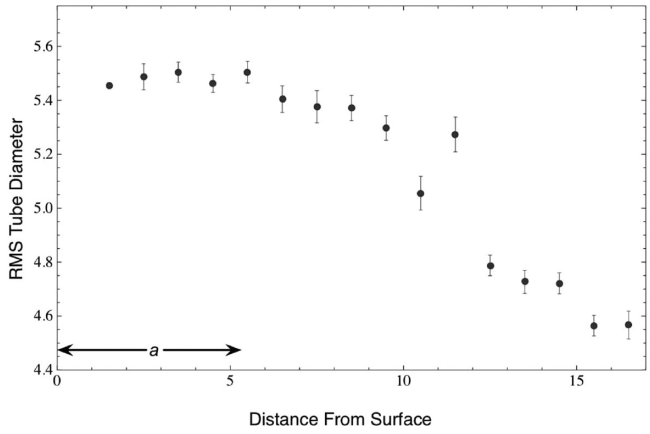

Figure 12. Tube size as a function of distance from the top or bottom of the simulation box. Average tube diameter indicated by a.

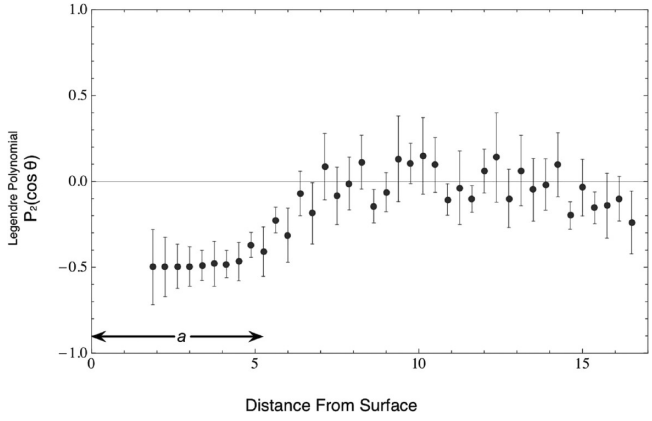

Figure 13. Average $\langle P_2(\cos\theta)\rangle$ versus distance from the nearest surface. Close to the surface, tube segments lie mainly parallel to the interface.

Tubes Near a Surface. Our nondestructive method for finding the tube is well suited to address effects of a free surface. Near a surface, changes to the size, shape, and orientation of the tube segments may be expected. To explore these effects, we equilibrated three rings of 800 monomers in a two-dimensionally periodic simulation box, after which we applied isoconfigurational averaging. The initial configuration is shown below in Figure 11.

The z direction was made finite by application of a repulsive potential at the top and bottom of the bounding box to confine the polymer chains to the melt. The simulation box was sized to be three times larger in the z direction than in x and y, so the chain segments in the middle would be representative of those found in a bulk polymer melt, unable to "feel" the surface.

Surface Effect Results. The first exploration of tube behavior near the surface is to examine tube size as a function of distance from the surface. Figure 12 shows the average tube size, calculated as the root-mean-square of the two shorter gyration tensor principal axes, versus distance from the nearest surface. The figure shows that tube size increases as the chain gets closer to the surface and smaller as the chain gets deeper in the melt. This observation can be explained in the following way: near the surface, each chain segment is not as evenly surrounded by neighboring chains, and there are of course no chains above the surface with which to entangle.

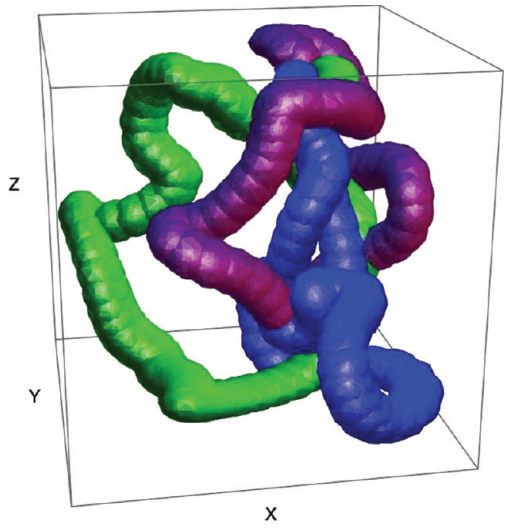

Figure 14. Ellipsiodal representation of three rings in a box finite in the z direction. The surface causes the confining tube to flatten and spread out parallel to the surface.

Another way to examine tube surface behavior is to look at the orientation distribution of tube segments. Each tube segment makes some angle θ with respect to the surface normal $\hat{z}$. A convenient measure of orientational anisotropy is the second Legendre polynomial $P_2(\cos\theta)$, averaged for tube segments at different distances from the box center:

$$P_2(\cos\theta) = \frac{1}{2}(3\cos^2\theta - 1) \quad (4)$$

The average $\langle P_2(\cos\theta)\rangle$ quantifies the tendency of a group of tube segments to be perpendicular or parallel to $\hat{z}$. So, if the tube segments are isotropic, the value of P_2 will fluctuate around zero. Whereas, if the segments tend to be parallel to the surface, $\langle P_2(\cos\theta)\rangle$ becomes negative as seen in Figure 13, which shows that the range of the surface-induced anisotropy is limited to about the mean tube diameter.

A final, more qualitative way to see the effect of a surface on the tube is to show the molecules in the same fashion as Figure 7, as selected gyration tensor ellipses. The result, Figure 14, shows the effect of the surface on the tube's shape, size, and orientation quantified in the above analyses.

CONCLUSIONS

We have demonstrated the usefulness and practicality of applying the isoconfigurational ensemble to a configuration of chains in order to explore the confining tube. The results noninvasively identify a smooth primitive path defined by the average monomer positions of multiple chain trajectories with different noise history starting from the same configuration.

In addition, the "cloud" of monomer positions surrounding the primitive path can be used to determine physical properties of the tube, including size, shape, and confining potential. Instead of inferring tube dimensions from distances between "kinks" in chain-shrinking methods, this data reveals local properties of the tube that vary continuously throughout the molecule.

By averaging over many possible trajectories to construct the primitive path, isoconfigurational averaging gives a smooth primitive path with a much shorter averaging time of only a few times the entanglement strand Rouse time τ_e, resulting in a view of the tube that is as instantaneous as possible.

We have applied the isoconfigurational averaging approach to a melt of one or more long entangled rings, topologically equilibrated by a hybrid Monte Carlo simulation in which chains are occasionally allowed to cross while maintaining their identities. The entanglement properties of long entangled rings are the same as for a melt of long entangled linear chains, but have the advantage for studies of tube properties that there are no tube renewal processes (no contour length fluctuations, constraint release, or reptation) when chain crossing moves are switched off.

We can determine various measures of the tube, namely the average cross-sectional diameter $\bar{a}$ (width of the confining potential), the effective step length $\tilde{a}$ on the primitive path, the mean-square end-to-end length of an entanglement strand N_e as determined from chain-shrinking algorithms, and the persistence length of the primitive path. All of these measures would be equivalent in the simple model of Doi and Edwards of the primitive path as a freely jointed random walk of step size a. For the model bead−spring system we studied, all these lengths are slightly different, consistent with a somewhat semiflexible primitive path. Finally, from a Gaussian fit to a probability distribution of monomer displacements from their mean positions, we show that the chain is confined to its tube by a harmonic potential.

We also applied our methods to investigate the effects of a surface on the tube. From this analysis it was found that the tube diameter smoothly increases by about 25%, and the surface effect is felt to about two tube diameters deep. The surface also induces anisotropy in the tube; segments within about a tube diameter of the surface tend to lie parallel to the surface.

In the present work, we identified points on the primitive path as the mean positions of the "clouds" of monomers in our isoconfigurational simulations. This identification results in a slight but annoying dependence of the primitive path length on the averaging time τ_a (scaling as $\tau_a^{-1/8}$), as a result of "corner-cutting" of the longitudinal motion of the chain in its tube (described in section X). A better method for determining the point on the primitive path corresponding to a "cloud" of monomer positions is to locate the point of maximum density in the cloud. This prescription properly identifies the center of a cloud even if the cloud is "bent around a corner", and will be exploited in our future work.

AUTHOR INFORMATION

Corresponding Author
*E-mail: stm9@psu.edu.

ACKNOWLEDGMENT

We thank Alexei Likhtman and Daniel Read for useful discussions, and NSF DMR-0907370 and ACS-PRF 49964-ND7 for support.

REFERENCES

(1) Doi, M.; Edwards, S. F. *The Theory of Polymer Dynamics*; Oxford University Press: Oxford, U.K., 1986.
(2) Lin, Y.-H. *Macromolecules* **1987**, *20*, 3080–3083.
(3) Kavassalis, T. A.; Noolandi, J. *Phys. Rev. Lett.* **1987**, *59*, 2674–2677.

(4) Fetters, L. J.; Lohse, D. J.; Richter, D.; Witten, T. A.; Zirke, A. *Macromolecules* **1994**, *27*, 996–998.
(5) Milner, S. T. *Macromolecules* **2005**, *38*, 4929–4939.
(6) Everaers, R.; Sukumaran, S. K.; Grest, G. S.; Svaneborg, C.; Sivasubramanian, A.; Kremer, K. *Science* **2004**, *303*, 823–826.
(7) Sukumaran, S. K.; Grest, G. S.; Kremer, K.; Everaers, R. *J. Polym. Sci., Part B: Polym. Phys.* **2005**, *43*, 917–933.
(8) Zhou, Q.; Larson, R. G. *Macromolecules* **2005**, *38*, 5761–5765.
(9) Shanbhag, S.; Larson, R. G. *Phys. Rev. Lett.* **2005**, *94*, 076001.
(10) Zhou, Q.; Larson, R. G. *Macromolecules* **2006**, *39*, 6737–6743.
(11) Kröger, M. *Comput. Phys. Commun.* **2005**, *168*, 209–232.
(12) Tzoumanekas, C.; Theodorou, D. N. *Macromolecules* **2006**, *39*, 4592–4604.
(13) Kremer, K.; Grest, G. S. *J. Chem. Phys.* **1990**, *92*, 5057–5086.
(14) Widmer-Cooper, A.; Harrowell, P. *J. Phys.: Condens. Matter* **2005**, *17*, S4025–4034.
(15) Widmer-Cooper, A.; Harrowell, P. *J. Non-Cryst. Solids* **2006**, *352*, 5098–5102.
(16) Read, D. J.; Jagannathan, K.; Likhtman, A. E. *Macromolecules* **2008**, *41*, 6843–6853.
(17) Milner, S. T.; Newhall, J. D. *Phys. Rev. Lett.* **2010**, *105*, 208302.
(18) Pant, P. V. K.; Theodorou, D. N. *Macromolecules* **1995**, *28*, 7224–7234.
(19) Karayiannis, N. C.; Mavrantzas, V. G.; Theodorou, D. N. *Phys. Rev. Lett.* **2002**, *88*, 105503.
(20) Morse, D. C.; Chung, J. K. *J. Chem. Phys.* **2009**, *130*, 224901.
(21) Qin, J.; Milner, S. T. To appear in *Soft Matter* **2011**.
(22) We gratefully acknowledge helpful conversations with Alexei Likhtman on this point.
(23) Shirvanyants, D.; Panyukov, S.; Liao, Q.; Rubinstein, M. *Macromolecules* **2008**, *41*, 1475–1485.